Combustion for propulsion

Analysis of the unstable acoustic frequencies of a Rijke tube

Group member
Harish REYYA

Master Aéronautique et Espace
École Centrale de Lyon
December 2022

Contents

List of Figures

List of Tables

1 Introduction

In this report we are trying to find the most unstable acoustic frequencies in a Rijke tube combustion problem. The configuration and governing equations are presented. We then apply a root-finding algorithm and from the resulting set extract the values of interest. We then analyse the structure of the standing pressure of these frequencies and in an attempt to push our investigation further we look at the effect of the imaginary component of the angular frequency.

This investigation is motivated by the need to have a better understanding of unstable acoustic modes in combustion chambers in order to take them into account in the design process. These modes can be destructive if not dealt with appropriately as seen in the Ariane II accident of 1980.

2 Theoretical reminders

We are interested in finding the unstable frequencies for the Rijke tube shown in figure 1. There we have two flow regions, hot and cold, separated by a flame. In this configuration an acoustic loop will generate acoustic waves in the tube which can be stable or unstable. The latter are of interest in in the aerospace industry due to there destructive nature (e.g. 1980 Ariane II accident).

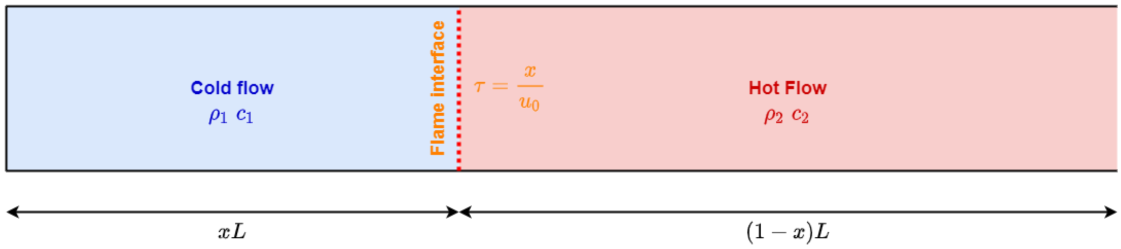

Figure 1: Configuration of the Rijke tube problem

The physical problem illustrated in figure 1 is defined by the parameters in table 1 and the acoustic modes are governed by equations 1 to 4 (where L_1 and L_2 are the lengths of the cold and hot sections respectively). Solving these determines the frequencies (f) that generate acoustic modes. These modes are unstable when the imaginary part of the angular frequency ($\omega = 2\pi \cdot f$) is positive.

Symbol	Value	Units	Variable description
L	1.783	m	Length of the tube
n	0.010	$-$	Normalised flame response
c_1	340.0	$m\,s^{-1}$	Speed of sound in first section
c_2	$2 \cdot c_1$	$m\,s^{-1}$	Speed of sound in second section
ρ_1	1.200	$kg\,m^{-3}$	Air density in first section
ρ_2	$\rho_1/4$	$kg\,m^{-3}$	Air density in second section
x	0.200	m	Position of the flame
u_0	20.00	$m\,s^{-1}$	Speed of flow in first section

Table 1: Variables of interest for Rijke tube problem

$$A_1^+ = A_1^- \tag{1}$$
$$A_2^- = -A_2^+ e^{2ik_2L_2} \tag{2}$$
$$A_1^+ cos(k_1L_1) = -iA_2^+ e^{ik_2L_2} sin(k_2L_2) \tag{3}$$
$$cos(k_2L_2)cos(k_1L_1) = \frac{\rho_2 c_2}{\rho_1 c_1} sin(k_2L_2)sin(k_1L_1)(1 + ne^{i\omega\tau}) \tag{4}$$

When equations 1 through 4 are resolve, we can use equation 5 to find the standing pressure inside the flow regions (i) of the tube. *Note :* in this equation be careful to distinguish between i the flow region and j the imaginary number. For the pressure in the hot flow region ($i = 2$) the the length of the cold flow region ($i = 1$) should be subtracted from the position (x).

$$P_i(x,t) = A_i^+ e^{jkx - j\omega t} + A_i^- e^{-jkx - j\omega t} \tag{5}$$

3 Methodology

To obtain the acoustic modes of the problem we recast equation 4 as follows,

$$g(\omega) = cos(k_2L_2)cos(k_1L_1) - \frac{\rho_2 c_2}{\rho_1 c_1} sin(k_2L_2)sin(k_1L_1)(1 + ne^{i\omega\tau}) \tag{6}$$

As such, we need to find the values of the angular frequency (ω) for which equation 6 is zero. This requires a root-finding method adapted for searches in the complex plane. For this we selected the Newton-Raphson method which is also appropriate for continuous and differentiable functions.

We developed a Python program (script provided) that implements this method in a subroutine by the same name. Its inputs are the expression whose root we want to find, the variable of interest, and an initial guess of said root. The subroutine evaluates the derivative of the expression and then iterates the Newton-Raphson method until the difference between two successive estimations is smaller than a critical value. We set this value as 0.01 to keep computation times reasonable.

Our search domain for this problem is situated between 200 and 20 000 Hz (the frequencies audible by most humans). To ensure that we find every root of equation 6 we can use each integer value in this range as an initial guess. This technique is time consuming, however, it allows us to globally apply a local-search method. A for-loop is used to complete this part of the program.

This produces a set of values containing the values that the Newton-Raphson method converges to for each initial guess. Figure 2a represents the real components of the values in this set and figure 2b shows those between 200 and 400 Hz. We observe that there are zones of constant value, these represent a root. Between two zones we find a region of perturbed values, in this area the Newton-Raphson method encountered difficulties converging to one value as the initial guess was located in between roots. The program processes the data series to extract the values of the constant zones.

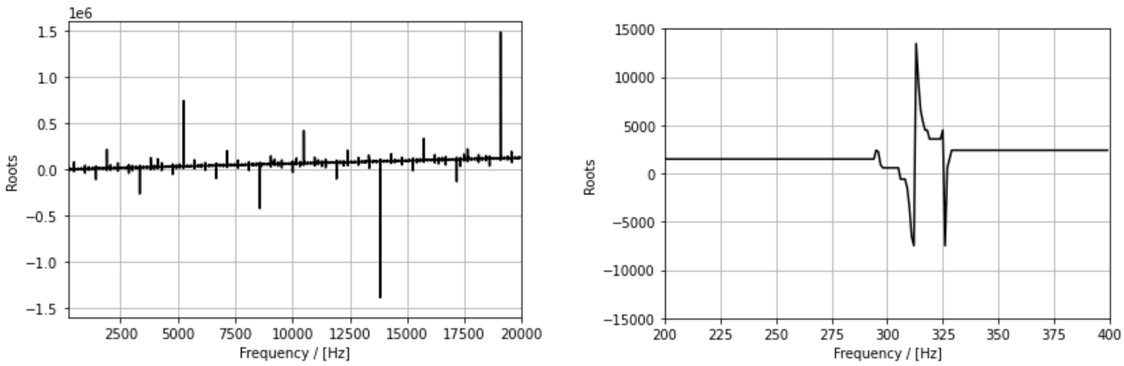

(a) Full range of frequencies

(b) Zoom between $f = 200$ and $400\,Hz$

Figure 2: Values found by the Newton-Raphson method (in real plane)

Once the roots of the problem have been extracted, we are interest in finding the once associated to the most unstable acoustic frequencies. These are the ones with a positive imaginary component. So, the program first sorts the data to find the roots satisfying this criterion. However, many of them have small imaginary components, some that are practically zero. Thus, we define the most unstable acoustic frequencies to be those whose positive imaginary component is greater than one.

With this completed, what remains is to find the tones associated with these frequencies using an online tone generator and to plot the standing pressure inside the tube using equations.

4 Results and analysis

For the analysis we limit ourselves to frequencies between 200 and 10 000 Hz, as past this limit the associated tones are above B8 (they are also irritating to the ear). Table 2 presents the most unstable acoustic frequencies found by the Python program described in the previous section. We recall that these are the ones whose imaginary component is greater than positive one.

Angular frequency (ω)	Real component (f)	Associated tone
$3582.51 + 1.06287j$	$570.17\,Hz$	$C\sharp5/D\flat5$
$15563.4 + 1.10179j$	$2477.0\,Hz$	$D\sharp7/E\flat7$
$23376.3 + 1.06489j$	$3720.5\,Hz$	$A\sharp7/B\flat7$
$35357.2 + 1.10092j$	$5627.3\,Hz$	$F8$
$54503.1 + 1.11078j$	$8674.4\,Hz$	Above $B8$
$62315.0 + 1.00010j$	$9917.9\,Hz$	Above $B8$

Table 2: Most unstable acoustic frequencies between 200 and 10 000 Hz

The next part of the results and analysis is to plot the structure of the standing pressure of the unstable acoustic frequencies inside the tube. For this we need values of amplitude for equations 1 through 4. Arbitrarily setting $A_1^+ = 1$ and using we immediately obtain the remaining amplitudes for a given angular frequency. The final part of the Python program accomplishes this task.

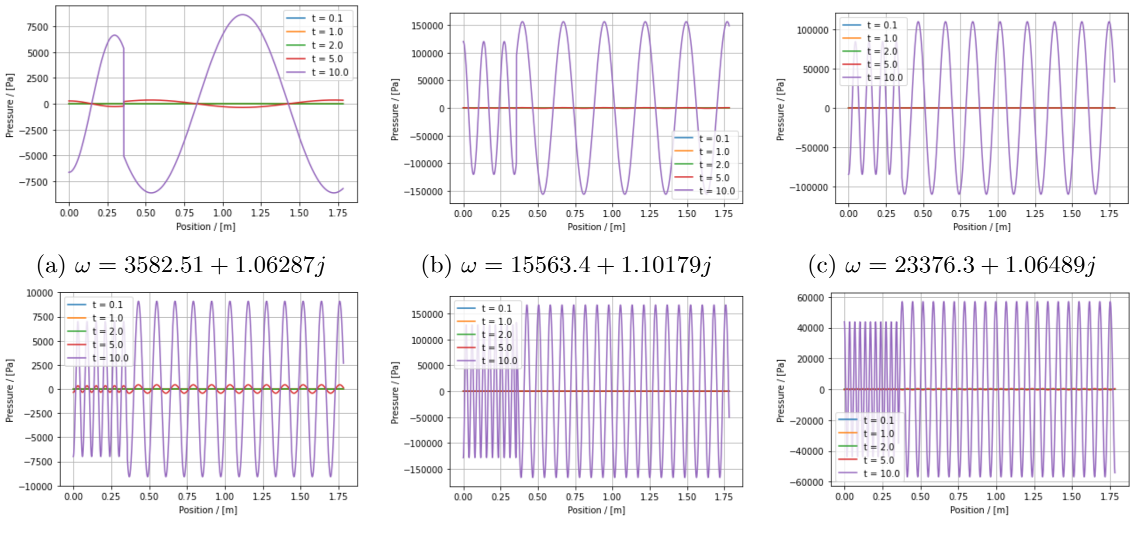

(a) $\omega = 3582.51 + 1.06287j$ (b) $\omega = 15563.4 + 1.10179j$ (c) $\omega = 23376.3 + 1.06489j$

(d) $\omega = 35357.2 + 1.10092j$ (e) $\omega = 54503.1 + 1.11078j$ (f) $\omega = 62315.0 + 1.00010j$

Figure 3: Structure of standing pressure at different times for most unstable acoustic frequencies

Figure 5 displays the structure of the standing pressure in the tube at different times for the most unstable acoustic frequencies given in table 2. It is clear that the amplitude increases with time, notably, after ten seconds the structure of the standing pressure dominants the ones from earlier times. This demonstrates the unstable nature of these acoustic frequencies.

To study the impact of the imaginary component of the angular frequency on the structure of the standing pressure we can take a look at figure 4. There we see the behaviour for an angular frequency with a positive imaginary component (4a), without an imaginary component (4b), and with a negative imaginary component (4c). Figure 4a is the same as figure 3a and that over time the structure becomes larger, thus is unstable. Then, for an angular frequency with no imaginary component, the structure fluctuates over time but remains low. Finally, for a negative angular frequency, the structure is constant over time and thus is stable. This shows the impact of the sign of the imaginary component of angular frequency on the the structure of the standing pressure.

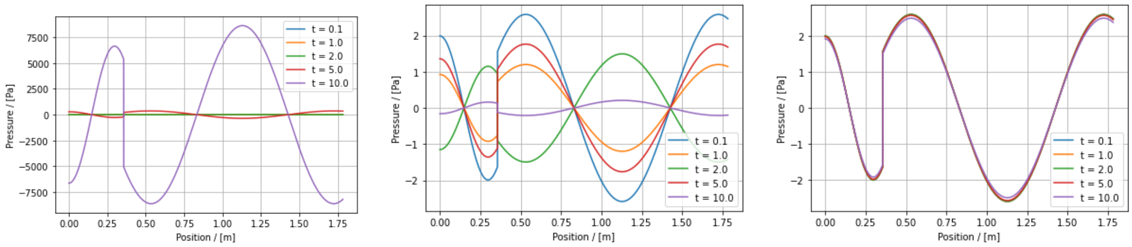

(a) $\omega = 35357.2 + 1.10092j$ (b) $\omega = 35357.2$ (c) $\omega = 35357.2 - 1.10092j$

Figure 4: Structure of standing pressure at different times for different acoustic frequencies

The unstable nature of the acoustic frequencies can be explained using the Rayleigh criterion. We recall that it states : for a localized heat source, if ϕ represents the phase between p_1 and $\dot{\omega}_{T1}$, the system will be unstable if $0 < \phi < \pi$ and it will be stable if $\pi < \phi < 2\pi$. This tells us that when the imaginary component of the angular frequency then $0 < \phi < \pi$ and so the system is unstable.

5 Conclusion

In this report we presented the main theoretical reminders for the creation of unstable acoustic modes in a Rijke tube (configuration in figure 1) as governed by equation 1 through 4. Then we devised a method to determine them which we implemented in a Python program (provided).

The program returned the most unstable acoustic frequencies between 200 and 10 000 Hz presented in table 2. Using an online tone generator we were able to provide the musical notes associated to the real component of these frequencies. Then, by selecting an arbitrary positive amplitude in the cold section of the tube ($A_1^+ = 1$) we resolved the set of governing equations and plotted the structure of the standing pressure that they generate in the Rijke tube.

We saw from the structures (figure 5) that for the unstable acoustic frequencies the associated standing pressure increases with time; to the point that after ten seconds the pressure is orders of magnitude greater than at the beginning. This demonstrates the unstable nature of these modes. We later related this behaviour to the Rayleigh criterion.

To push our investigation further we compared the influence of the imaginary component of the angular frequency on the structure of the standing pressure (figure 4). There we observed that for a positive imaginary value the evolution of the structure in time was unstable and increasing. For a zero value, the evolution was unstable but shows no growth. And for a negative value, the evolution was entirely stable - no growth nor decay and no change of peak position with time. The effect of the imaginary part could potentially be explored further by looking into the relationship between its magnitude and the growth rate of the structure over time. This could eventually lead to an empirical relation between the two quantity.

Lastly, the Python program was time-consuming to execute when looking for roots using the Newton-Raphson method. This is because we applied the method to each integer frequency value in our range to ensure that we obtained all the roots of equation 6. This was a way of disguising a local-search algorithm as a global one. It would be more appropriate to apply a global method.